C. R. Mecanique 339 (2011) 727–742

Contents lists available at ScienceDirect

Comptes Rendus Mecanique

www.sciencedirect.com

Geometrically non-linear steady state periodic forced response of a clamped–clamped beam with an edge open crack

El bekkaye Merrimi [a,*], Khalid El bikri [a], Rhali Benamar [b]

[a] Université Mohammed V-Souissi, Ecole normale superieure de l'enseignement technique Rabat, B.P. 6207, Rabat Instituts, Morocco
[b] Ecole Mohammadia d'ingenieurs, departement des EGT, Av. Ibn Sina, Agdal, Rabat, Morocco

ARTICLE INFO

Article history:
Received 19 May 2011
Accepted after revision 25 July 2011
Available online 8 September 2011

Keywords:
Vibrations
Non-linear forced vibrations
Cracked beam

ABSTRACT

The present work is concerned with the study of the geometrically non-linear steady state periodic forced response of a clamped–clamped beam containing an open crack. The model based on Hamilton's principle and spectral analysis, previously used to investigate various non-linear vibration problems, is used here to determine the effect of the excitation frequency and level of the applied harmonic force, concentrated at the cracked beam middle span, on its dynamic response at large vibration amplitudes. The formulation uses the "cracked beam functions", denoted as 'CBF', previously defined in recent works, obtained by combining the linear theory of vibration and the linear fracture mechanics theory. The crack has been modelled as a linear spring which, for a given depth, the spring constant remains the same for both directions. The results obtained may be used to detect cracks in vibrating structures, via examination of the qualitative and quantitative changes noticed in the non-linear dynamic behaviour, which is commented in the conclusion.

1. Introduction

Many engineering components used in the aeronautical, aerospace and naval construction industries are considered by designers as vibrating structures, operating under a large number of random cyclic stresses. Consequently, it is natural to expect fatigue crack initiation and propagation to occur in critically stressed zones of such structures, in particular in the neighbourhood of local or general resonances, as can be seen by the reader interested in more details in Refs. [1–8]. Non-linear analysis is therefore necessary in such situations to predict accurately the geometrically non-linear structural behaviour at large vibration amplitudes, and establish appropriate design criteria [9,10].

The topic of non-linear vibration of beams is of continuing interest, due to their frequent use as experimental test pieces [11] and because they constitute one of the simplest cases of a continuous system, since their motion is represented by one-dimensional partial differential equation in space. Hence, they may be very useful for exploring and validating new theoretical and numerical approaches in the field of non-linear structural dynamics.

As stated in Ref. [12], non-linear vibration analysis is an important current theme. This topic is not recent, the early studies dating from the 19th century, but it is currently of renewed interest because of the need to optimise the commonly used structures subjected to high excitation levels or to treat the many unsolved problems involving contact, rubbing vibration, fracture, fatigue, noise and vibration control. For linear vibration, the range of techniques and software dedicated to experimental or digital analysis is very broad and corresponds to a large number of problems of acoustic radiation and structural vibration. Linear theoretical concepts are clear and many tools, now classical and very well known, are available.

* Corresponding author.
E-mail address: merbe2004@yahoo.fr (E.b. Merrimi).

1631-0721/$ – see front matter
doi:10.1016/j.crme.2011.07.008

Nomenclature

L	length of the beam
b	width of the beam
h	thickness of the beam
S	the dimensional surface $[0, b] \times [0, h]$
I_z	area moment of inertia of the beam cross-section
a	crack depth
β	non-dimensional flexibility induced by the presence of the crack
M_f	bending moment
$W(x,t)$	transverse displacement at abscises on the beam $W(x,t) = w(x)\Phi(t)$
$W^*(x,t)$	non-dimensional transverse displacement at abscises x on the beam
ν	Poisson's ratio
ρ	mass per unit volume of the beam
E	Young's modulus
K_I	stress intensity factor for mode I
x_0	position of the crack
k_{ij}	rigidity tensor
m_{ij}	mass tensor
b_{ijkl}	non-linearity tensor
k^*_{ij}, m^*_{ij}, b^*_{ijkl}	general terms for the non-dimensional rigidity tensor, mass tensor and non-linearity tensor, respectively
ω	frequency parameter
ω^*	non-dimensional frequency parameter
ω_e	excitation frequency
ω^*_e	non-dimensional excitation frequency
T	kinetic energy
V_b, V_a	bending and axial strain energy of the beam respectively
V_c	crack strain energy due to the crack
$F(x,t)$	harmonic excitation force
V_f	potential energy associated to the force $F(x,t)$
δ	Dirac function

However, if one of the non-linear effects enters into play, due for example to the geometrical or material non-linearity, or to the boundary conditions, many types of difficulties appear, especially for problem identification or calculation, and a considerable research effort is still needed, in order to develop appropriate and efficient models, including the most significant effects in the situation under examination. These include the non-linear increase in resonant frequency and stresses with the amplitude of vibration. The significant contributions of the higher modes in the non-linear steady state periodic forced response is also necessary to take into account in engineering applications, especially those related to structural safety, because of their effects on the non-linear strains and stresses estimation. Such an effort will have impact on the design of high-performance structures, since it will provide engineers and designers with appropriate tools ensuring more accuracy and efficiency in current situations.

On the other hand, cracks growing over the time in a structural member, as the load reversals continue, may reach a point at which it becomes a threat to the structural integrity. In this context, numerous catastrophic failures have been reported in the last few decades. For this reason, designers have to make fatigue resistance one of their most important concerns, in order to ensure that all of the components of the structure have a well estimated fatigue life, especially when crack initiation and propagation are distinct possibilities. Also, high-performance structures, which must have a low weight, and consequently, are designed with the smallest possible thickness, may be subjected to high level working loads, especially in severe environment, which induce large vibration amplitudes. Also, non-destructive testing and control methods have become a focus of substantially growing research efforts. Indeed, new and advanced inspection techniques are required to accurately monitor the state of this type of structural failure at earlier stages, so that in the event of development of any crack, it can be detected, located and if possible repaired before it propagates and impair the safety of these structures. Among these newly emerging techniques, modal analysis and vibration monitoring techniques are being explored by many researchers in order to define efficient procedures for non-destructive examination. It is well known that the dynamic behaviour of a structure is dependent on its structural properties, i.e. the mass, stiffness and damping distributions. Therefore, any subsequent change in one or many of these properties due to the presence of a crack should induce a change in the dynamic characteristics, such as the natural frequencies, displacements, strains/stresses, mode shapes and damping [13].

The development of techniques based on modal analysis of cracked members may be of a substantial value, since this may avoid the dismantling of the structure, allowing in-service testing. Hence, to overcome the engineering problems mentioned above, a considerable amount of work has been carried out by researchers for modelling a transverse crack normal to the surface of a structure. This has ranged from simple slots cut into beams and reduction in the local elastic modulus [14,15], to spring hinge model combined with the fracture mechanics results [16–23].

The various attempts made in the last few decades by Benamar and co-workers [24–32], to describe in a unified manner the geometrically non-linear free and forced vibrations of thin straight structures, such as beams, plates and circular cylindrical shells, using Hamilton's principle and spectral analysis, show that the concept of normal modes of vibration in the non-linear case may be very useful and yields a deep insight into the structural dynamic behaviour. This has been shown theoretically by the considerable computing time saving and the relative mathematical simplicity of the non-linear semi-analytical models developed, in which the linear mode shape bases are used to expand the unknown displacement series.

The objective of this work is to present a semi-analytical method for determination of the forced non-linear flexural response of clamped–clamped beams with an edge open crack at large vibration amplitudes. The formulation is established

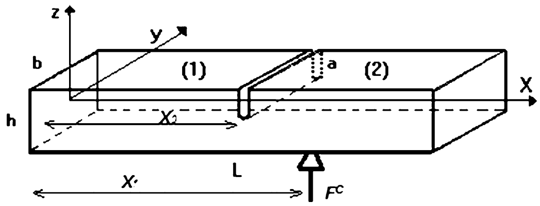

Fig. 1. Physical model of the cracked beam with a harmonic excitation force.

using Hamilton's principle and spectral analysis and admissible functions, called "cracked beam functions", denoted in [32] as 'CBF', which satisfy the natural and geometrical end conditions, as well as the inner boundary conditions at the crack location.

2. General formulation

2.1. Semi-analytical model for the non-linear forced flexural vibration of clamped–clamped beams with an edge crack at high excitation levels, inducing large vibration amplitudes

Consider the beam shown in Fig. 1, loaded by the concentrated harmonic force applied at the point x_f and having a uniform transverse surface crack of depth a located at the position x_0 accounted from the left end of the beam. The stored strain energy of the cracked beam at large vibration amplitudes can be obtained through summation of the stored bending strain energy V_b, the stored strain energy at the crack location V_c [32], the stored axial strain energy V_a induced by large displacement amplitudes, and the potential energy associated to the applied force $F(x,t)$. Their respective expressions are given as follows:

$$V_b = \frac{EI}{2}\int_0^L \left(\frac{\partial^2 W}{\partial x^2}\right)^2 \mathrm{d}x \tag{1}$$

$$V_c = \frac{(EI)^2}{2K_f}\left(\frac{\partial W^2}{\partial x^2}\right)^2_{x=x_0} \tag{2}$$

$$V_a = \frac{ES}{8L}\left\{\int_0^L \left(\frac{\partial W}{\partial x}\right)^2 \mathrm{d}x\right\}^2 \tag{3}$$

Upon assuming harmonic motion and expanding the displacement W in the form of a finite series, one obtains:

$$W(x,t) = w(x)\sin\omega t = a_i w_i(x)\sin\omega t \tag{4}$$

The physical force $F(x,t)$ excites the modes of the structures via a set of generalised forces $f_i(t)$ depending on the expression for F, the excitation point for the concentrated force considered here, and the mode considered [29]. The potential energy associated to the force $F(x,t)$ is given by:

$$V_f = -\int_0^l F(x,t)W(x,t)\,\mathrm{d}x \tag{5}$$

The total beam strain energy can be written as:

$$V = V_b + V_a + V_c + V_f \tag{6}$$

The dynamic behaviour for a conservative system may be obtained by application of Hamilton's principle, which can be written as:

$$\delta\int_0^{2\pi/\omega} (V - T)\,\mathrm{d}t = 0 \tag{7}$$

The kinetic energy is given by:

$$T = \frac{1}{2}\rho S\int_0^l \left(\frac{\partial W}{\partial t}\right)^2 \mathrm{d}x \tag{8}$$

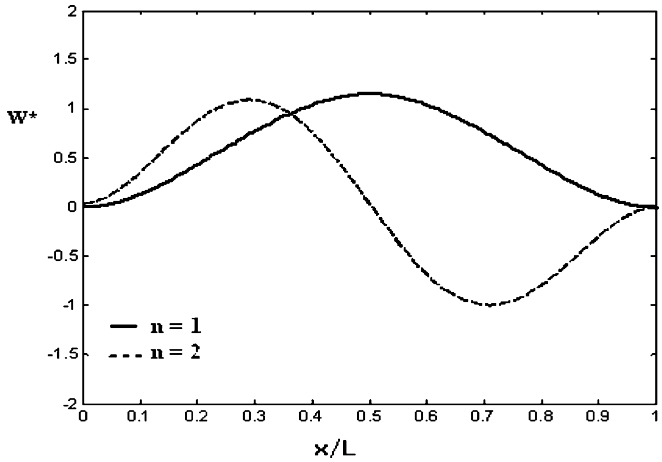

Fig. 2. CBF for $n = 1, 2$ and $a/h = 0.3$.

The expressions used for V_b, V_a, V_f, V_c and T depend on the problem considered and the hypotheses adopted. $W(x,t)$ in (4) depends on $\{w_i^{CBF},\ i = 1, \ldots, n\}$, which represents a set of n spatial trial functions called cracked beam functions and denoted as 'CBF'. These functions, plotted below in the case of a crack of relative depth $a/h = 0.3$, for $n = 1, 2$ (Fig. 2), have been defined in [32–36] using fracture mechanics and linear vibration theories.

The discretized expressions for the potential and kinetic energies are then obtained as:

$$V_b = \frac{1}{2} a_i a_j k_{ij}^{b^{CBF}} \sin^2(\omega t) \tag{9}$$

$$V_c = \frac{1}{2} a_i a_j k_{ij}^{c^{CBF}} \sin^2(\omega t) \tag{10}$$

$$V_a = \frac{1}{2} a_i a_j a_k a_l b_{ijkl}^{CBF} \sin^4(\omega t) \tag{11}$$

$$T = \frac{1}{2} \omega^2 a_i a_j m_{ij}^{CBF} \cos^2(\omega t) \tag{12}$$

Thus, using the notation of (1)–(4), one obtains:

$$k_{ij}^{CBF} = EI\left\{ \int_0^l \left(\frac{\partial^2 w_i^{CBF}}{\partial x^2}\right)\left(\frac{\partial^2 w_j^{CBF}}{\partial x^2}\right) \mathrm{d}x + \frac{EI}{K_f} \frac{\partial^2 w_i^{CBF}}{\partial x^2}\bigg|_{x=x_0} \frac{\partial^2 w_j^{CBF}}{\partial x^2}\bigg|_{x=x_0} \right\} \tag{13}$$

$$b_{ijkl}^{CBF} = \frac{ES}{4L} \int_0^l \frac{\partial w_i^{CBF}}{\partial x} \frac{\partial w_j^{CBF}}{\partial x} \,\mathrm{d}x \int_0^l \frac{\partial w_k^{CBF}}{\partial x} \frac{\partial w_l^{CBF}}{\partial x} \,\mathrm{d}x \tag{14}$$

$$m_{ij}^{CBF} = \rho s \int_0^l w_i^{CBF} w_j^{CBF} \,\mathrm{d}x \tag{15}$$

The beam is excited by a concentrated harmonic force F^c applied at the point x_f. Then, one can write:

$$F^c(x,t) = F^c \delta(x - x_f) \sin(\omega_e t) \tag{16}$$

where δ is the Dirac function.

The discretized expression for the potential energy associated to the force $F^c(x,t)$ is given by:

$$V_f^c = -a_i f_i^c \sin^2(\omega_e t) \tag{17}$$

where:

$$f_i^c = F^c w_i^{CBF}(x_f) \tag{18}$$

Using Hamilton's principle and the matrix notation, the process leads to n non-linear algebraic equations for the unknown coefficients a_i which can be written in a matrix form as follows:

$$\big([\mathbf{K}] - \omega^2[\mathbf{M}]\big)\{\mathbf{A}\} + \frac{3}{2}\big[\mathbf{B}(\mathbf{A})\big]\{\mathbf{A}\} = \{\mathbf{F}\} \tag{19}$$

Eq. (19) is formally identical to that obtained in Refs. [27] and [30] for the non-linear forced response of uniform beams. ω corresponds to the given excitation frequency.

2.2. Evaluation of the non-dimensional coefficients

To obtain non-dimensional parameter, one puts:

$$w_i(x) = h w_i^*\left(\frac{x}{L}\right) = h w_i^*\big(x^*\big) \tag{20}$$

$$\frac{k_{ij}^{CBF}}{k_{ij}^{*CBF}} = \frac{EIh^2}{L^3} \tag{21}$$

$$\frac{m_{ij}^{CBF}}{m_{ij}^{*CBF}} = \rho S h^2 L \tag{22}$$

$$\frac{b_{ijkl}^{CBF}}{b_{ijkl}^{*CBF}} = \frac{EIh^2}{L^3} \tag{23}$$

$$\frac{f_i^c}{f_i^{c*}} = \frac{EIh^2}{L^3} \tag{24}$$

which leads to:

$$\frac{\omega_e^2}{\omega_e^{*2}} = \frac{EI}{\rho S L^4} \tag{25}$$

where k_{ij}^{*CBF}, b_{ijkl}^{*CBF}, and m_{ij}^{*CBF} are non-dimensional generalised parameters given by:

$$k_{ij}^{*CBF} = \int_0^1 \frac{\partial^2 w_i^{*CBF}}{\partial x^{*2}} \frac{\partial^2 w_j^{*CBF}}{\partial x^{*2}}\,\mathrm{d}x^* + \beta \frac{\partial^2 w_i^{*CBF}}{\partial x^{*2}}\bigg|_{x_0^*} \frac{\partial^2 w_j^{*CBF}}{\partial x^{*2}}\bigg|_{x_0^*} \tag{26}$$

$$b_{ijkl}^{*CBF} = \alpha \int_0^1 \frac{\partial w_i^{*CBF}}{\partial x^*} \frac{\partial w_j^{*CBF}}{\partial x^*}\,\mathrm{d}x^* \int_0^1 \frac{\partial w_k^{*CBF}}{\partial x^*} \frac{\partial w_l^{*CBF}}{\partial x^*}\,\mathrm{d}x^* \tag{27}$$

$$m_{ij}^{*CBF} = \int_0^1 w_i^{*CBF} w_j^{*CBF}\,\mathrm{d}x^* \tag{28}$$

in which β is a non-dimensional parameter expressed as:

$$\beta = \frac{EI}{K_f L} \tag{29}$$

For a uniform beam with a rectangular cross-section, $\alpha = 3$, since in this case, ($h^2 S/I = 12$).

Eq. (19) can be rewritten in non-dimensional form as:

$$\big(\big[\mathbf{K}^*\big] - \omega^{*2}\big[\mathbf{M}^*\big]\big)\{\mathbf{A}\} + \frac{3}{2}\big[\mathbf{B}^*(\mathbf{A})\big]\{\mathbf{A}\} = \big\{\mathbf{F}^*\big\} \tag{30}$$

Or using tensorial notation:

$$a_i k_{ir}^{*CBF} + \frac{3}{2} a_i a_j a_k \big(b_{ijkr}^{*CBF}\big) - \omega_e^{*2} a_i m_{ir}^{*CBF} = f_i^{c*}, \quad r = 1, \ldots, n \tag{31}$$

The dimensional force f_i^{c*} corresponds to the concentrated force applied at x_f on the beam, given in Eqs. (18) and (24).

3. The non-linear frequency response function in the neighbourhood of the first non-linear mode shape of clamped–clamped cracked beams under a harmonic excitation force, based on the single mode approach

In this section, a solution of the non-linear amplitude equation obtained in the model presented above, based on the single mode assumption, is proposed. The objective is to validate the model, and to obtain a simple formula for the non-linear forced response of clamped–clamped beams with an edge crack in the neighbourhood of its fundamental resonance.

Eq. (19) represents a set of differential equations in which $\{\mathbf{F}\}$ is a column vector of generalised forces. This equation appears as a generalisation to the non-linear case of the classical linear forced response equation, very well known in linear modal analysis theory, to which the term $3/2[\mathbf{B}(\mathbf{A})]\{\mathbf{A}\}$ corresponding to the non-linear geometrical rigidity is added. On the other hand, if only one mode is assumed, as will be considered below, Eq. (19) reduces to:

$$a_1 k_{11}^{*CBF} + \frac{3}{2} a_1^3 \left(b_{1111}^{*CBF}\right) - \omega_e^{*2} a_1 m_{11}^{*CBF} = f^{c*CBF} \tag{32}$$

in which m_{11}, k_{11} and b_{1111} are the mass, rigidity and non-linearity terms corresponding to the first mode respectively. Putting:

$$\left(\omega_l^*\right)^2 = \frac{K_{11}^{*CBF}}{m_{11}^{*CBF}} \tag{33}$$

where ω_l^* is the linear natural frequency parameter, Eq. (32) can be written as:

$$\left(\frac{\omega_e^*}{\omega_l^*}\right)^2 = \frac{3}{2} \frac{b_{1111}^{*CBF}}{k_{11}^{*CBF}} a_1^2 - \frac{f^{c*CBF}}{a_1 k_{11}^{*CBF}} + 1 \tag{34}$$

The last equation enables one to plot the non-linear frequency response function, i.e. W_{max}^*, which is directly related to the coefficient a_1, as a function of the excitation frequency ω_e, of the cracked beam, characterised by the parameters k_{11} and b_{1111}, in the neighbourhood of the first non-linear mode shape for various levels of the harmonic excitation force, defined by f^{c*CBF}. If the amplitude of the excitation is taken equal to 0, the backbone curve, corresponding to the free vibration case, is obtained, as illustrated in the next subsection.

3.1. Free vibration

Identical clamped–clamped steel beams, containing a crack of different depths, located at their mid-span, have been considered here, with the following material and geometrical properties: Young's modulus $E = 200$ GPa, material density $\rho = 7850$ kg/m^3, thickness $h = 10$ mm, width $b = 20$ mm, and length $L = 300$ mm.

If free vibrations are considered, the dependence of the non-linear frequency on the non-dimensional vibration amplitude is obtained from Eq. (34), by putting $f^{c*CBF} = 0$. The corresponding backbone curves are plotted in Fig. 3, in the neighbourhood of the first non-linear mode shape of the clamped–clamped beam, for various values of the crack depth. As may be expected, a hardening type of non-linearity, similar to that mentioned in Ref. [32] for the first non-linear mode shape of a clamped–clamped beam, is observed. This is explained by the fact that the deflection shape associated to the mode shape produces induced in-plane membrane stresses, tensile in nature that effectively stiffens the beam at large vibration amplitudes. It should be noticed that the presence of the crack magnifies this effect, especially when the crack depth increases.

3.2. Forced vibrations

In Fig. 4, the non-linear frequency response functions of the cracked beam examined, with a depth crack of 0.3, are plotted in the neighbourhood of the first non-linear mode shape, for various levels of the harmonic excitation force. The qualitative behaviour shown in Fig. 4, obtained from Eq. (34), which is of the hardening type, is characteristic for the non-linear frequency response functions of systems with a cubic non-linearity. It includes multivalued regions in which the jump phenomena, very well known in non-linear frequency response testing, may occur [24–32]. As no damping is involved, the curves remain open, and the dashed curve, in the middle, correspond to the backbone curve. In Fig. 5, the non-linear frequency response curves, of a C–C beam with an edge crack at the middle of its span, are plotted for various crack depths. It can be seen that the increase in the crack depth induces an increase in the hardening effect, which may be attributed to the reason mentioned in the above subsection.

4. The non-linear frequency response functions of clamped–clamped cracked beams under a harmonic excitation force, based on a multimode approach, in the neighbourhood of the first non-linear mode shape

In spite of the simplicity of the single mode approach and its ability to predict quite accurately the non-linear frequency response curve in the neighbourhood of the resonance considered, as shown in the previous subsection, it remains insufficient in a sense that it does not give any information about the amplitude dependence of the response deflection shape,

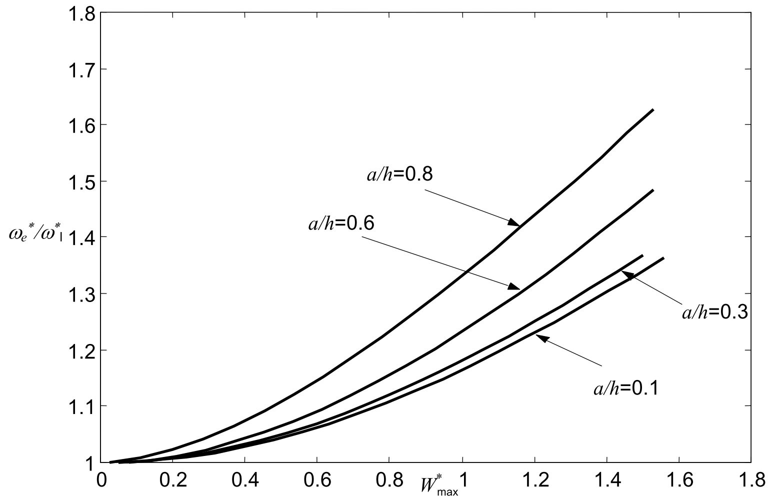

Fig. 3. Backbone curves of clamped–clamped cracked beams, in the vicinity of the first mode, for various crack depths (0.3, 0.6, 0.8).

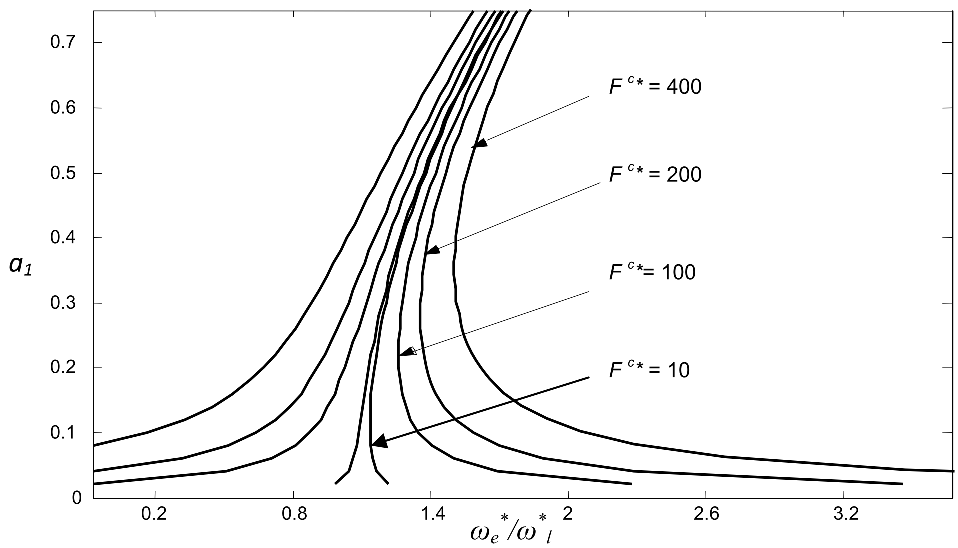

Fig. 4. Non-linear frequency response functions, based on the single mode approach, of a C–C beam, with an edge crack located at $x_0 = L/2$, crack depth $= 0.3h$, for various levels of the harmonic excitation forces.

which has been shown both experimentally and theoretically to occur at large vibration amplitudes [11,24–26]. This non-linear aspect, often ignored by the analysts, is practically important for estimating accurately the non-linear strain and stress distributions, which are quantities of crucial effect with respect to structural safety and fatigue life prediction. In order to remedy this insufficiency, a multimode approach to the non-linear steady state periodic forced response of cracked beams is developed here, based on an analysis similar to that presented in Ref. [30], with the objective of predicting the non-linear frequency response function of the beam, not only at its maximum deflection point, i.e., the beam middle span when considering the first resonance, but also for the whole span of the beam. Numerical results obtained for various values of the crack depth and levels of the excitation force will be presented via solution in each case of the set of non-linear algebraic equations, i.e. Eq. (30). The method of solution adopted in the present section is based on the explicit formulation developed and applied to solve various non-linear vibration problems [30–32,37], which allows an easy and simplified calculation of the non-linear steady state periodic forced response of cracked beams.

4.1. Numerical details

Consider the non-linear forced response of a clamped–clamped cracked beam in the neighbourhood of its first resonant frequency; following the basic function choice adopted in the previous section, to obtain the values of the linear rigidity matrix k_{ij}^{*CBF} and the non-linear geometrical rigidity tensor b_{ijkl}^{*CBF} of the first non-linear mode shape of the cracked C–C beam

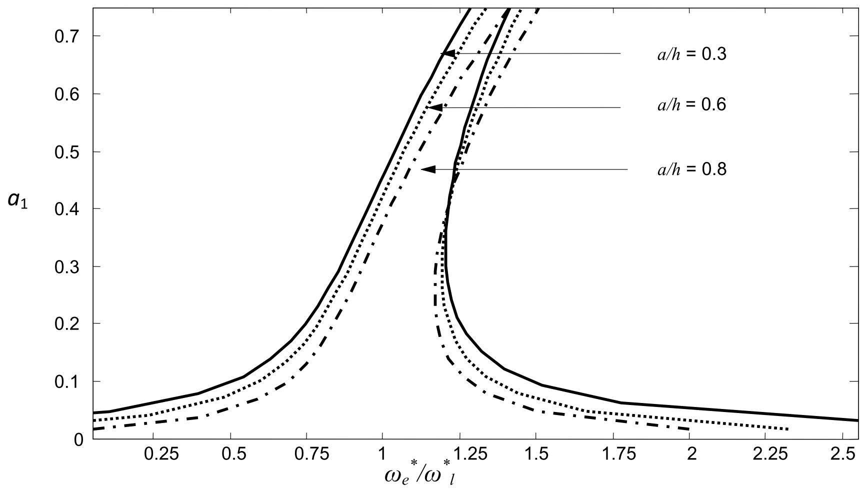

Fig. 5. Non-linear frequency response functions, based on the single mode approach, of a C–C beam, with an edge crack located at $x_0 = L/2$, for $F^{c*} = 200$, for various crack depths $(0.3, 0.6, 0.8)$.

Table 1
First non-linear mode shape of cracked beam, $a/h = 0.1$.

W^*_{max}	0.79575821E−01	0.47617067E+00	0.94572196E+00
ω^*_{nl}/ω^*_l	1.00053987	1.03942916	1.14844776
a_1	0.05	0.3	0.6
a_3	0.10800000E−05	0.10112615E−02	0.73288085E−02
a_5	0.73254800E−06	0.12639556E−03	0.98559574E−03
a_7	−0.55800000E−06	0.20158496E−04	0.16127465E−03
a_9	0.59800000E−06	0.47003343E−05	0.38290176E−04
a_{11}	−0.10800000E−07	0.19925048E−05	0.16291913E−04

examined, the first six normalised symmetric 'CBF' $w_1^{*CBF}, w_3^{*CBF}, \ldots, w_{11}^{*CBF}$ are used first. The functions w_i^{*CBF} have been normalised in such a manner that the obtained mass matrix equals the identity matrix. Calculations of the corresponding integrals, defined in Eqs. (26)–(28), have been performed numerically, using the Simpson's rule.

4.2. Brief review of the explicit procedure of solution

To illustrate the main idea behind the simplified approach of solution of the amplitude equation (31) used in what follows, we present here in Table 1, the results obtained via iterative solution of the non-linear algebraic system (30) for the first non-linear mode shape of a C–C cracked beam, with $a/h = 0.1$, previously published in [32]. It can be seen in this table, that the contribution a_1 of the first basic function, which is the first C–C 'CBF', remains predominant for the whole range of vibration amplitudes considered, compared to the contributions of the other functions. So, the contribution coefficient vector $\{\mathbf{A}\}$ defined in Section 2.1 by $\{\mathbf{A}\}^T = [a_1\ a_3\ \ldots\ a_{11}]$ can be written as $\{\mathbf{A}\}^T = [a_1\ \varepsilon_3\ \ldots\ \varepsilon_{11}]$ in which ε_i, representing the ith basic function contribution, may be considered as small, compared to a_1, for $i = 3, 5, \ldots, 11$. Since the non-linearity parameters b_{ijkl}^{*CBF} defined in (27) are of the same order of magnitude, due to the above observation, some terms may be neglected in the non-linear expression $a_i a_j a_k b_{ijkr}^{*CBF}$ in Eq. (31), which leads to a simple formulation, defined as below.

Reconsidering Eq. (31):

$$a_i k_{ir}^{*CBF} + \frac{3}{2} a_i a_j a_k \left(b_{ijkr}^{*CBF}\right) - \omega_e^{*2} a_i m_{ir}^{*CBF} = f_i^{c*}, \quad i = 1, \ldots, n \tag{35}$$

the simplified formulation is based on an approximation which consists of neglecting in the expression $a_i a_j a_k b_{ijkr}^{*CBF}$ of Eq. (35), first, second and third order terms with respect to ε_i, i.e. terms of the type $a_1^2 \varepsilon_k b_{11kr}^{*CBF}$, of the type $a_1 \varepsilon_j \varepsilon_k b_{1jkr}^{*CBF}$, or of the type $\varepsilon_i \varepsilon_j \varepsilon_k b_{ijkr}^{*CBF}$, so that the only remaining term is $a_1^3 b_{111r}^{*CBF}$. In the neighbourhood of the first resonance, the above equation becomes:

$$\left(k_{ir}^{*CBF} - \omega_e^{*2} m_{ir}^{*CBF}\right)\varepsilon_i + \frac{3}{2} a_1^3 b_{111r}^{*CBF} = f_i^{c*} \quad \text{for } r = 3, 5, \ldots, 11 \tag{36}$$

In which the repeated index i is summed over the range $\{1, 3, \ldots, 11\}$. Since the use of linear 'CBF' as basic functions leads to diagonal mass and rigidity matrices, Eq. (36) can be written as:

Table 2
Clamped–clamped cracked beam subjected to a harmonic excitation force – explicit solution $a/h = 0.3$.

ω_e^*/ω_l^*	W_{max}^*/h	$d^2W/dx^2(0)$	a_1	ε_3	ε_5	ε_7	ε_9	ε_{11}	Residual
9.288E−01	3.620E−01	1.76E+01	2.24E−01	4.50E−06	7.06E−04	−5.48E−07	7.43E−05	1.55E−07	1.482E−05
1.009E+00	4.421E−01	1.84E+01	2.74E−01	8.87E−06	1.34E−03	−1.01E−06	1.32E−04	3.27E−07	1.357E−04
1.083E+00	5.219E−01	1.92E+01	3.24E−01	1.59E−05	2.27E−03	−1.68E−06	2.16E−04	5.41E−07	6.815E−04
1.230E+00	6.797E−01	3.438E−01	4.240E−01	4.385E−05	5.303E−03	−3.79E−06	4.813E−04	1.214E−06	6.924E−03
1.245E+00	7.109E−01	3.519E−01	4.340E−01	4.822E−05	5.712E−03	−4.07E−06	5.161E−04	1.303E−06	8.367E−03

Table 3
Clamped–clamped cracked beam subjected to a harmonic excitation force – explicit solution $a/h = 0.6$.

ω_e^*/ω_l^*	W_{max}^*/h	$d^2W/dx^2(0)$	a_1	ε_3	ε_5	ε_7	ε_9	ε_{11}	Residual
1.025E+00	4.010E−01	2.20E+01	1.54E−01	1.11E−05	5.07E−04	−1.36E−06	1.05E−05	4.44E−07	1.340E−04
1.065E+00	4.346E−01	2.29E+01	1.64E−01	1.37E−05	6.22E−04	−1.65E−06	1.16E−05	5.36E−07	4.964E−04
1.104E+00	4.680E−01	2.38E+01	1.74E−01	1.68E−05	7.53E−04	−1.97E−06	1.29E−05	6.40E−07	1.453E−03
1.142E+00	5.012E−01	2.48E+01	1.84E−01	2.03E−05	9.01E−04	−2.34E−06	1.44E−05	7.58E−07	3.613E−03
1.181E+00	5.341E−01	2.58E+01	1.94E−01	2.44E−05	1.07E−03	−2.74E−06	1.60E−05	8.88E−07	7.967E−03

$$\left(k_{rr}^{*CBF} - \omega_e^{*2} m_{rr}^{*CBF}\right)\varepsilon_r + \frac{3}{2}a_1^3 b_{111r}^{*CBF} = f_r^{c*} \quad \text{for } r = 3, 5, \ldots, 11 \tag{37}$$

In which no summation is involved. The last system permits one to obtain explicitly the modal contributions $\varepsilon_3, \varepsilon_5, \ldots, \varepsilon_{11}$ of the symmetric basic functions corresponding to a given value of the assigned first basic function contribution a_1 as follows:

$$a_1 = \frac{f_1^{c*} - \frac{3}{2}a_1^3 b_{1111}^{*CBF}}{k_{11}^{*CBF} - \omega_e^{*2} m_{11}^{*CBF}} \quad \text{for 1st linear mode} \tag{38}$$

$$\varepsilon_r = \frac{f_r^{c*} - \frac{3}{2}a_1^3 b_{111r}^{*CBF}}{k_{rr}^{*CBF} - \omega_e^{*2} m_{rr}^{*CBF}} \quad (r = 3, 5, \ldots, 11) \tag{39}$$

In the above equation, the ε_r's, for $r > 1$, depend on the classical modal parameters m_{rr}^{*CBF}, k_{rr}^{*CBF}, the non-linear modal parameters b_{111r}^{*CBF}, the assigned first function contribution a_1, calculated via Eq. (38), the non-linear frequency parameter ω_e^*, and the amplitude of the excitation force f_1^{c*}.

Expression (39) is an explicit simple formula allowing calculation of the higher mode contributions to the non-linear frequency response function, in the vicinity of the first non-linear mode shape. The non-linear beam deflection $W_{nl1}^*(x, a_1)$, for a given assigned value a_1, is then obtained as a series involving the beam modal parameters depending on the first six symmetric C–C 'CBF' w_1^{*CBF}, $w_3^{*CBF}, \ldots, w_{11}^{*CBF}$ given by:

$$W_{nl}^*(x, a_1) = \frac{f_1^{c*} - \frac{3}{2}a_1^3 b_{1111}^{*CBF}}{(k_{11}^{*CBF} - \omega_e^{*2} m_{11}^{*CBF})} w_1^{*CBF}(x) + \frac{f_3^{c*} - \frac{3}{2}a_1^3 b_{1113}^{*CBF}}{(k_{33}^{*CBF} - \omega_e^{*2} m_{33}^{*CBF})} w_3^{*CBF}(x) + \cdots + \frac{f_{11}^{c*} - \frac{3}{2}a_1^3 b_{11111}^{*CBF}}{(k_{1111}^{*CBF} - \omega_e^{*2} m_{1111}^{*CBF})} w_{11}^{*CBF}(x) \tag{40}$$

The range of validity, in terms of amplitudes of vibration or levels of excitation, of this expression is limited, due to the assumptions made to simplify the non-linear system. However, it remains quite interesting, as shown below, by substituting the numerical solutions obtained from Eq. (40) in the amplitude equation and calculating the residual. The range of validity has been determined by fixing the residual at 10^{-3}, as shown below.

4.3. Numerical results obtained by the explicit formulation

Replacing in Eq. (40) the clamped–clamped modal parameters by their values, computed numerically, leads to the following expression for the non-linear amplitude dependent beam response deflection shape $W_{nl1}^*(x, a_1)$, for a given value a_1 of the first mode contribution, in the case of crack depths $a/h = 0.3$:

$$\begin{aligned} W_{nl103}^*(x, a_1) = {} & \frac{f_1^{c*} - \frac{3}{2}a_1^3 2245.70}{(1268.93 - \omega_e^{*2})} w_1^{*CBF}(x) + \frac{f_3^{c*} - \frac{3}{2}a_1^3 590.98}{(3803.53 - \omega_e^{*2})} w_3^{*CBF}(x) + \frac{f_5^{c*} + \frac{3}{2}a_1^3 2233.40}{(13878.50 - \omega_e^{*2})} w_5^{*CBF}(x) \\ & + \frac{f_7^{c*} - \frac{3}{2}a_1^3 479.35}{(39943.79 - \omega_e^{*2})} w_7^{*CBF}(x) + \frac{f_9^{c*} + \frac{3}{2}a_1^3 970.19}{(84859.44 - \omega_e^{*2})} w_7^{*CBF}(x) + \frac{f_{11}^{c*} + \frac{3}{2}a_1^3 709.17}{(173881.31 - \omega_e^{*2})} w_{11}^{*CBF}(x) \end{aligned} \tag{41}$$

In Tables 2 to 4, numerical results obtained from Eq. (40) for the modal contributions to the non-linear amplitude dependent beam deflection shape $W_{nl1}^*(x, a_1)$, for various values of the first mode contribution a_1, determined using the amplitude and frequency of the excitation force via Eq. (38), of the cracked C–C beam, are summarised, for different values

Table 4
Clamped–clamped cracked beam subjected to a harmonic excitation force – explicit solution $a/h = 0.8$.

ω_e^*/ω_l^*	W_{max}^*/h	$d^2W/dx^2(0)$	a_1	ε_3	ε_5	ε_7	ε_9	ε_{11}	Residual
1.036E+00	3.174E−01	1.77E+01	1.64E−01	1.09E−04	2.65E−03	−8.55E−06	−1.31E−04	2.72E−06	2.222E−04
1.071E+00	3.360E−01	1.93E+01	1.74E−01	1.43E−04	3.21E−03	−1.02E−05	−1.58E−04	3.25E−06	6.384E−04
1.105E+00	3.544E−01	2.04E+01	1.84E−01	1.86E−04	3.85E−03	−1.22E−05	−1.88E−04	3.85E−06	1.566E−03
1.139E+00	3.726E−01	2.19E+01	1.94E−01	2.45E−04	4.57E−03	−1.43E−05	−2.21E−04	4.52E−06	3.417E−03
1.173E+00	3.906E−01	2.28E+01	2.04E−01	3.24E−04	5.40E−03	−1.67E−05	−2.59E−04	5.26E−06	6.815E−03

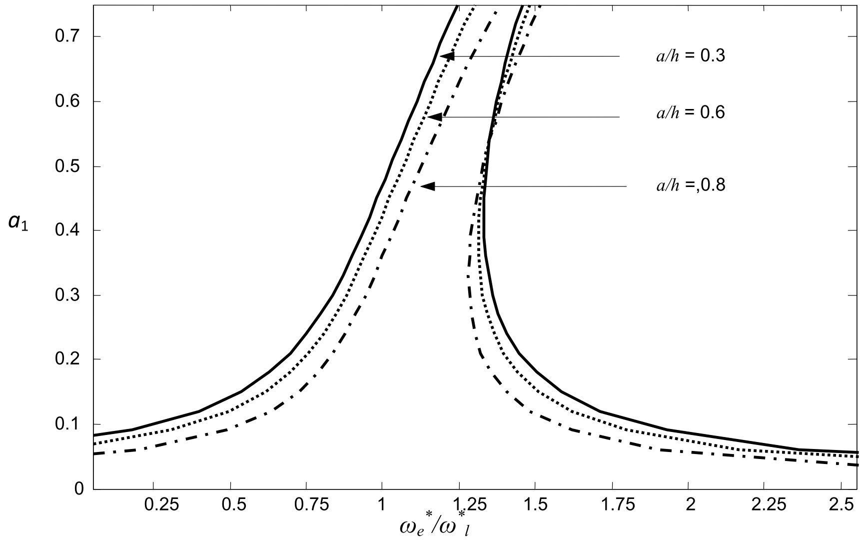

Fig. 6. Non-linear frequency response functions, based on the single mode approach, of a C–C beam, with an edge crack located at $x_0 = L/2$, for $F^{c*} = 400$, for various crack depths $(0.3, 0.6, 0.8)$.

of the crack depth. The values of $\varepsilon_3, \varepsilon_5, \ldots, \varepsilon_{11}$ obtained from Eq. (39), are given, with the corresponding maximum non-dimensional vibration amplitude at the beam middle span, and the corresponding values of ω_e^*/ω_l^* and the curvature calculated at $x^* = 0$. Also, care has been taken before exploiting the proposed formulation to determine accurately the range of validity of the numerical results obtained. To do so, Eq. (30) has been written as follows:

$$\left(\left[\mathbf{K}^*\right] - \omega_e^{*2}\left[\mathbf{M}^*\right]\right)\{\mathbf{A}\} + \frac{3}{2}\left[\mathbf{B}^*(\mathbf{A})\right]\{\mathbf{A}\} - \left\{\mathbf{F}^*\right\} = \{0\} \tag{42}$$

Then, the numerical solutions obtained via Eq. (40) have been substituted in Eq. (42) and calculation has been made of the resulting right hand side, i.e. a vector {Residual}. The norm of the vector {Residual} has been calculated in each case, and summarised in Tables 2–4. The limit of this norm, called the residual, fixed at 10^{-3} has permitted to determine the range of validity of the solutions obtained for each value of the frequency and level of the excitation force.

In Figs. 5 and 6, the non-linear frequency response functions, based on the single mode approach, of a C–C beam, with an edge crack located at $x_0 = L/2$, excited by a harmonic concentrated force, are plotted for various crack depths $(0.3, 0.6, 0.8)$ and two levels of the excitation force $F^{c*} = 200$ and $F^{c*} = 400$. It may be noticed that increasing the crack depth increases the hardening effect and the narrowness of the response function curves. In Fig. 7, comparison is made between the non-linear frequency response functions, obtained by the single mode approach and the multimode approach, of a C–C beam, with an edge crack located at $x_0 = L/2$, $F^{c*} = 200$, $a/h = 0.3$. The two curves are very close to each other for maximum vibration amplitude W_{max}^*/h up to 0.3 and slight differences start to appear for higher vibration amplitudes.

Fig. 8 shows the non-linear frequency response functions, based on the multimode approach, of a C–C beam, with an edge crack located at $x_0 = L/2$, $F^{c*} = 200$, for various crack depths $(0.3, 0.6, 0.8)$. It can be seen that for an identical level of excitation, the hardening effect is much more accentuated for a crack depth of 0.8, compared to that obtained for a crack depth of 0.3. This remark may be useful as an indication of the crack propagation when analysing experimental data. In Fig. 9, comparison is made of the non-linear frequency response functions, obtained for two excitation levels, i.e. $F^{c*} = 100$ and $F^{c*} = 200$, based on the multimode approach, of a C–C beam, with an edge crack located at $x_0 = L/2$, $a/h = 0.3$.

In Fig. 10, the curvature distributions are given, associated to the non-linear deflection response function, of a C–C beam with an edge crack, subjected to a concentrated force ($F^{c*} = 200$), for various crack depths $(0.3, 0.6, 0.8)$ and a maximum non-dimensional deflection $W_{max}^*/h = 0.4$.

In Figs. 11 to 13, the curvature distributions, associated to the non-linear deflection response function, of a C–C beam with an edge crack, subjected to a concentrated force ($F^{c*} = 200$), for various crack depths $(0.3, 0.6, 0.8)$ and maximum

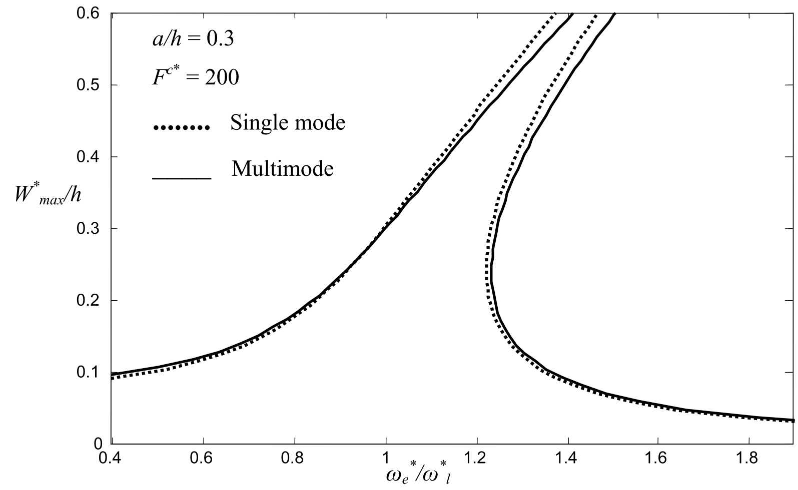

Fig. 7. Comparison of the non-linear frequency response functions of a C–C beam, with an edge crack located at $x_0 = L/2$, $F^{c*} = 200$, $a/h = 0.3$, obtained by the single mode approach and the multimode approach.

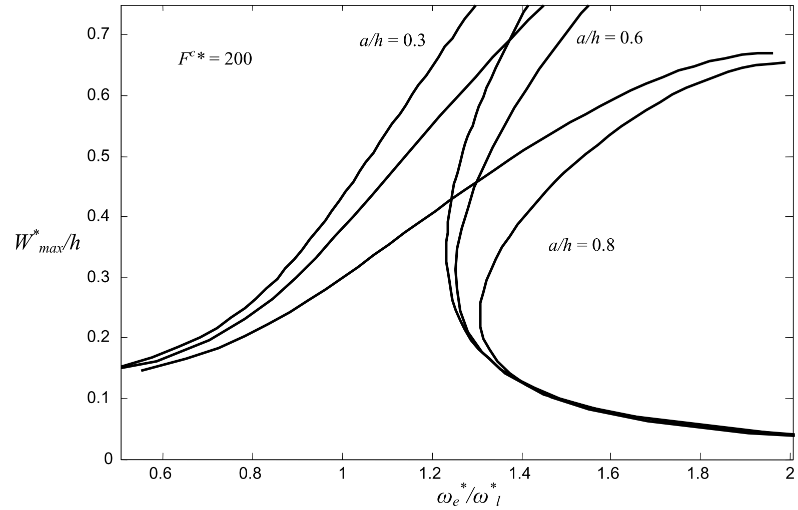

Fig. 8. Non-linear frequency response functions, based on the multimode approach, of a C–C beam, with an edge crack located at $x_0 = L/2$, $F^{c*} = 200$, for various crack depths $(0.3, 0.6, 0.8)$.

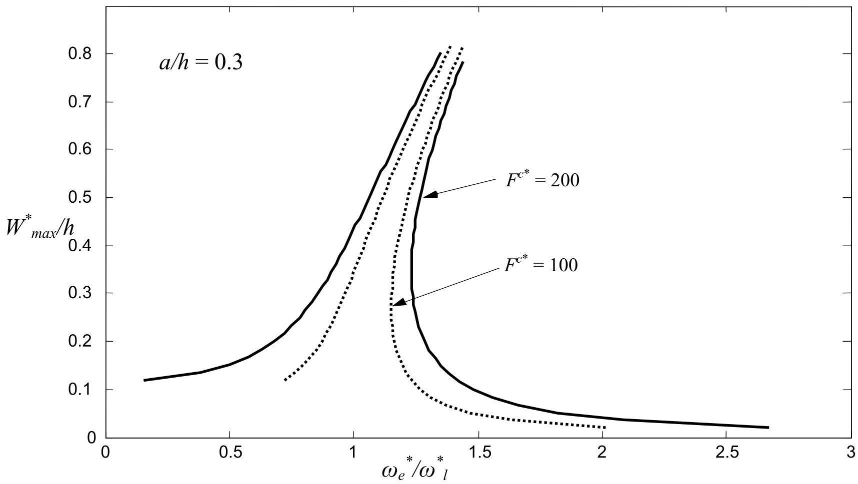

Fig. 9. Comparison of non-linear frequency response functions, based on the multimode approach, of a C–C beam, with an edge crack located at $x_0 = L/2$, $a/h = 0.3$, for two excitation levels.

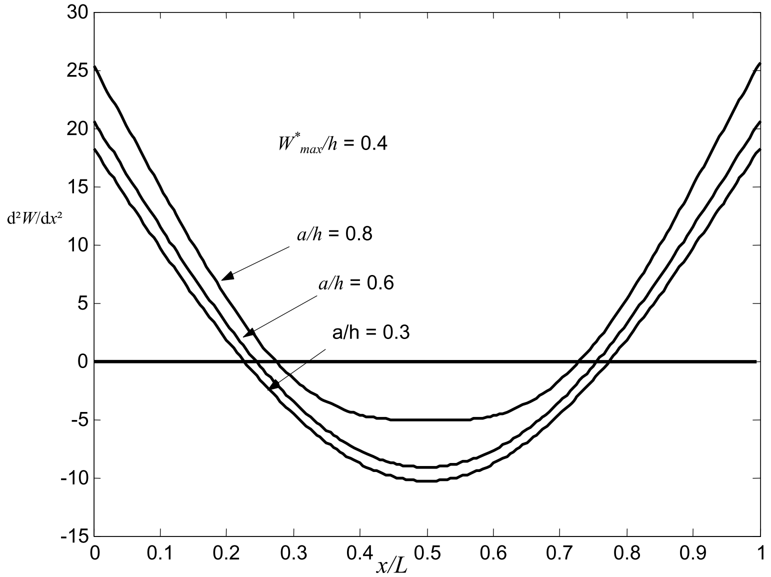

Fig. 10. Curvature distributions, associated to the non-linear deflection response function, of a C–C beam with an edge crack, subjected to a concentrated force ($F^{c*} = 200$), for various crack depths (0.3, 0.6, 0.8) and a maximum deflection $W^*_{max}/h = 0.4$.

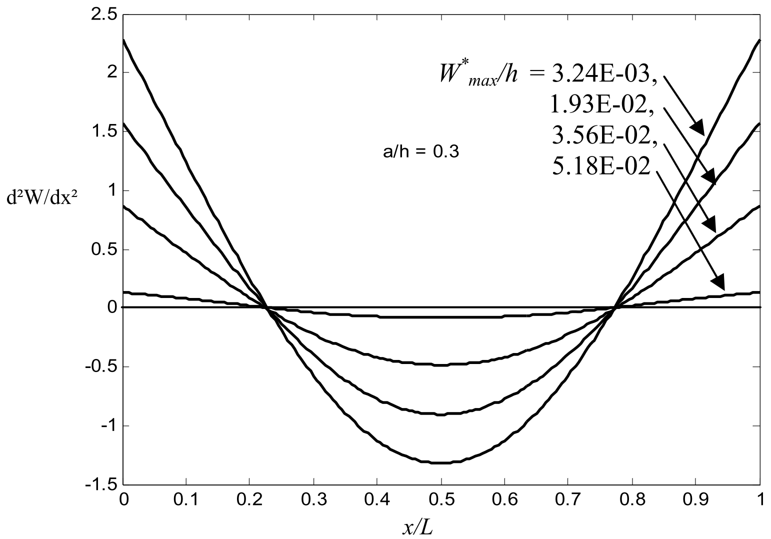

Fig. 11. Curvature distributions, associated to the non-linear deflection response function, of a C–C beam with an edge crack located at $x_0 = L/2, a/h = 0.3$, subjected to a concentrated force ($F^{c*} = 200$), for various values of the maximum deflections $W^*_{max}/h = 3.24\text{E}-03$, 1.93E−02, 3.56E−02, 5.18E−02.

deflections $W^*_{max}/h = 3.24\text{E}-03$, 1.93E−02, 3.56E−02, 5.18E−02. Fig. 14 shows a comparison of the values of the curvature at the clamps, $x = 0$, of a C–C beam with an edge crack, subjected to a concentrated harmonic force ($F^{c*} = 200$), for various values of the crack depth. The corresponding values are summarised in Table 5, in which the percentage of additional increase of curvatures (PAIC) at the clamps, due to the non-linearity, with increasing the vibration amplitude, are given for various values of the crack depths, showing a significant non-linear effect, which has to be taken into account for estimating accurately the non-linear stresses in cracked beams.

In Figs. 15 and 16, the corresponding distributions of curvatures, directly related to strains and stresses, are given, showing that the difference between the single mode and the multimode stress estimates may be significant at high vibration amplitudes, as has been mentioned above. The curves given have been limited to the domain of validity of the formulation adopted for solving the non-linear amplitude equation but higher differences in the curvature estimates are expected to occur for higher vibration amplitudes. However, it may be seen that this effect, which does not exceed 6% for $W^*_{max}/h = 0.67$ and crack depth $a/h = 0.3$, reaches 14% in Fig. 16 corresponding to $W^*_{max}/h = 0.4$ and $a/h = 0.8$.

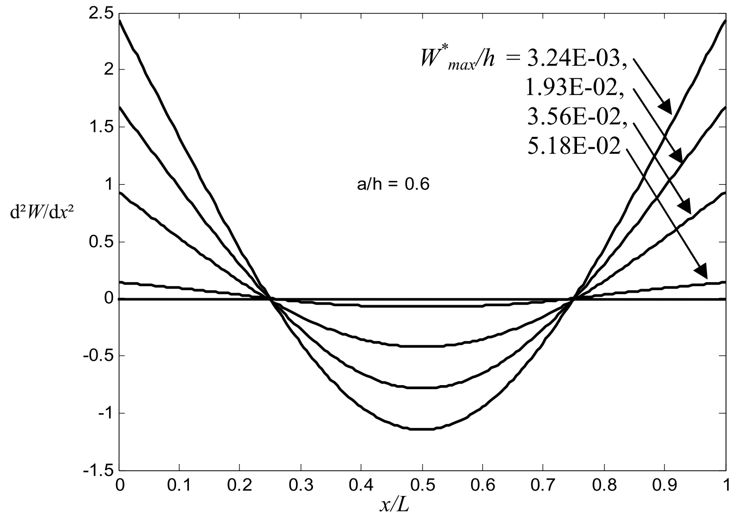

Fig. 12. Curvature distributions, associated to the non-linear deflection response function, of a C–C beam with an edge crack located at $x_0 = L/2$, $a/h = 0.6$, subjected to a concentrated force ($F^{c*} = 200$), for various values of the maximum deflections $W^*_{max}/h = 3.24\text{E}{-}03$, 1.93E−02, 3.56E−02, 5.18E−02.

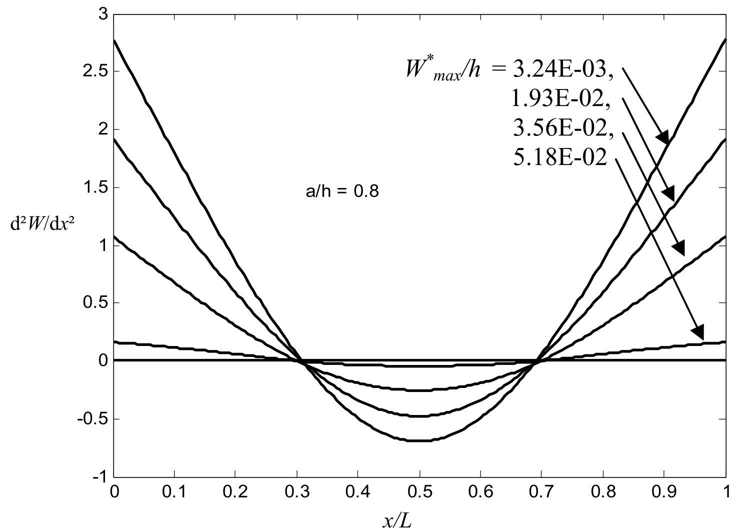

Fig. 13. Curvature distributions, associated to the non-linear deflection response function, of a C–C beam with an edge crack located at $x_0 = L/2$, $a/h = 0.8$, subjected to a concentrated force ($F^{c*} = 200$), for various values of the maximum deflections $W^*_{max}/h = 3.24\text{E}{-}03$, 1.93E−02, 3.56E−02, 5.18E−02.

5. Conclusion

The purpose of the present work was the investigation to the case of the steady state periodic forced vibrations of clamped–clamped beams with an edge open crack, which has been modelled, for a given crack depth, by a spring constant having the same value for both directions of vibration. The cracked beam is excited by a harmonic concentrated force, applied at the beam mid-span. The excitation point was chosen in such a manner to ensure that the first mode is predominant in the beam response, in order to make it possible to justify the assumptions adopted in the solution of the non-linear amplitude equation.

The formulation has led to a set of non-linear algebraic equation involving the mass matrix, the linear rigidity matrix, the non-linear rigidity tensor, and a right hand side made of the vector of generalised forces due to the applied excitation force. To solve this system, two procedures of solution have been adopted:

1) The single mode approach, assuming that only the first mode is involved in the response, has been first adopted. The frequency response curves have been obtained, using this assumption, giving the displacement W_{max} at the beam mid-span as a function of the excitation frequency, for different values of the crack depth and various levels of the excitation

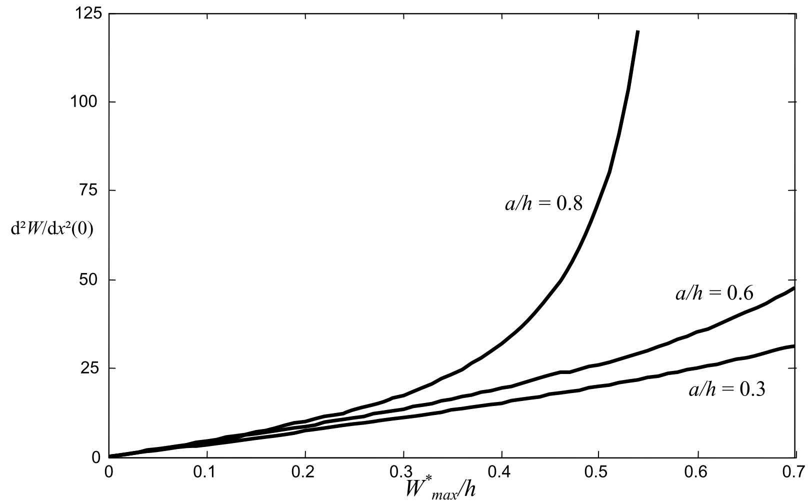

Fig. 14. Comparison of the values of the curvature at the clamps, $x = 0$, of a C–C beam with an edge crack, subjected to a concentrated harmonic force ($F^{c*} = 200$), for various values of the crack depth $(0.3, 0.6, 0.8)$.

Table 5
Percentage of additional increase of curvatures (PAIC) at the clamps, due to the non-linearity, with increasing the vibration amplitude, for various values of the crack depths.

	Curvature at $x = 0$		
	$W_{max}/h = 0.1$	$W_{max}/h = 0.4$	PAIC
$a/h = 0.3$	1.28	18.42	57%
$a/h = 0.6$	1.35	20.34	63%
$a/h = 0.8$	2.26	25.60	77%

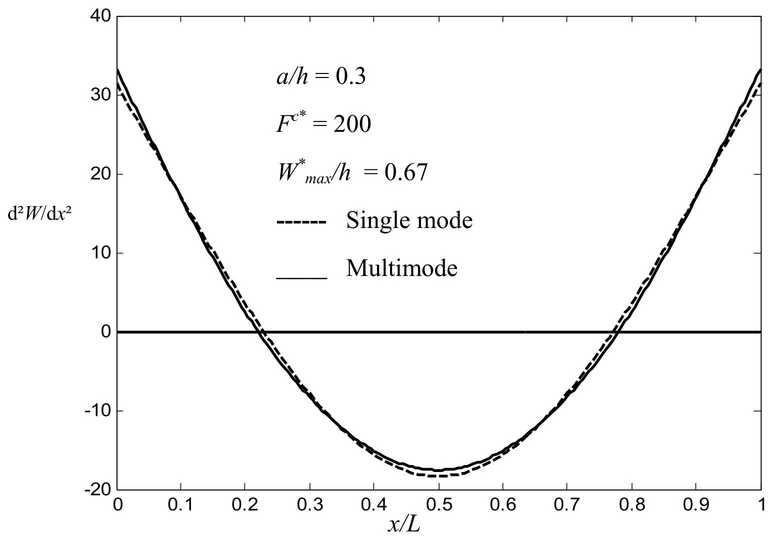

Fig. 15. Comparison of the curvature distributions of a C–C beam, with an edge crack located at $x_0 = L/2$, $F^{c*} = 200$, $a/h = 0.3$, $W^*_{max}/h = 0.67$ obtained by the single mode approach and the multimode approach.

forces. All curves exhibit the classical behaviour, of the hardening type, of non-linear systems with a cubic non-linearity, with multi-valued regions, corresponding physically to the possible occurrence of the jump phenomenon.

2) The second procedure of solution of the non-linear amplitude equation, based on a multimode approach, combined with the so-called first formulation, developed for the first time in [28], and then applied to different vibration problems in [29–32] has been then applied. This second procedure permitted explicit calculation of the non-linear frequency response function, for the excited cracked beam, involving not only the fundamental mode, but also the contributions of

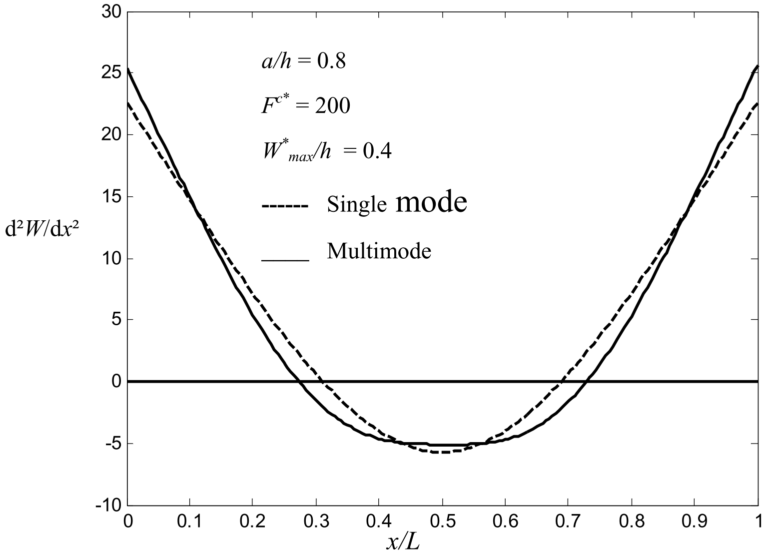

Fig. 16. Comparison of the curvature distributions of a C–C beam, with an edge crack located at $x_0 = L/2$, $F^{c*} = 200$, $a/h = 0.8$, $W^*_{max}/h = 0.4$ obtained by the single mode approach and the multimode approach.

the higher modes, which leads to a change in the response deflection shape, with the amplitude of vibration, inducing, among other affects, a non-linear increase of curvatures, with increasing the level of the excitation.

The analysis of the numerical results obtained for various crack depths and excitation levels, illustrated by the figures given, leads to the following qualitative remarks:

- The hardening type of non-linearity of the clamped–clamped cracked beam, excited by a harmonic concentrated force, is increased in a remarkable way with increasing the crack depth. This is due to the decrease in the thickness of the beam at crack location, which increases its flexibility.
- An increase of curvature with the crack depth, especially at the clamped end of the beam.

Appendix A

The tensor b^{*CBF}_{ijkl} is defined by:

$$b^{*CBF}_{ijkl} = \alpha \int_0^l \frac{\partial w^{*CBF}_i}{\partial x^*} \frac{\partial w^{*CBF}_j}{\partial x^*} \, dx^* \int_0^l \frac{\partial w^{*CBF}_k}{\partial x^*} \frac{\partial w^{*CBF}_l}{\partial x^*} \, dx^* = \alpha RAG(i,j).RAG(k,l) \tag{A.1}$$

For a clamped–clamped cracked beam, the matrices $RAG_{0.3}$ corresponding to a crack depth $a/h = 0.3$, is given numerically (for $i, j = 1, 3, 5, 7, 9, 11$) by:

$$RAG_{0.3}(i,j) = \begin{bmatrix} 27.36 & 7.20 & -27.22 & 5.84 & -11.82 & -8.64 \\ 7.20 & 41.14 & 11.29 & -29.63 & 3.06 & -11.76 \\ -27.22 & 11.30 & 103.86 & 16.19 & -47.50 & 3.22 \\ 5.84 & -29.63 & 16.19 & 197.76 & 27.75 & -65.70 \\ -11.82 & 3.06 & -47.50 & 27.75 & 301.02 & 52.70 \\ -8.64 & -11.76 & 3.22 & -65.70 & 52.70 & 385.03 \end{bmatrix} \tag{A.2}$$

References

[1] N.E. Dowling, Mechanical Behaviour of Materials, Engineering Methods for Deformation, Fracture, and Fatigue, Prentice–Hall Int. Ed., 1993.
[2] A.D. Dimarogonas, Crack identification in aircraft structures, in: 1st National Aircraft Conf., Greece, 1982.
[3] C. Hahin, J.M. South, J. Mohammadi, R.K. Polepeddi, Damage in steel bridges, J. Struct. Eng. 119 (1) (1993) 150–167.
[4] T.G. Chondros, A.D. Dimarogonas, Identification of cracks in circular plates welded at the contour, in: A.S.M.E. Design Eng. Technical Conf., 79-DET-106, St Louis, 1979.
[5] T.G. Chondros, A.D. Dimarogonas, Identification of cracks in welded joints of complex structures, Journal of Sound and Vibration 69 (1980) 531–538.
[6] J.Y. Guigne, A.S.J. Swamidas, J. Guzzwell, Modal information from acoustic measurements for fatigue crack detection applications, in: Proceedings 11th Int. Conf. on Offshore Technology and Arctic Eng., vol. I, Part B, 1992.

[7] A.J. Dentoras, A.D. Dimarogonas, Fatigue crack propagation in resonating structures, Eng. Fracture Mech. 34 (3) (1989) 721–728.
[8] P. Rabbe, C. Amzallag, Etude de l'amorçage des fissures et de la vitesse de fissuration par fatigue de quelques aciers inoxidables austénitiques, Revue de Métallurgie (1974) 931–941.
[9] C. Mei, K.R. Wentz, Large-amplitude random response of angle-ply laminated composite plates, American Institute of Aeronautics and Astronautics, Journal 20 (1982) 1450–1458.
[10] R.G. White, Developments in the acoustic fatigue design process for composite aircraft structures, Composite Structures 16 (1990) 171–192.
[11] M.M. Bennouna, R.G. White, The effect of large vibration amplitudes on the dynamic strain response of a clamped–clamped beam with consideration of fatigue life, Journal of Sound and Vibration 96 (1984) 281–308.
[12] F. Pérignon, Vibration forcée des structures minces, élastiques, non linéaires, Thèse, université Aix-Marseille II, 2004.
[13] R.D. Adams, P. Cawley, C.J. Pey, B.J. Stone, A vibration technique for non-destructively assessing the integrity of structures, J. Mech. Eng. Sci. 20 (1978) 93–100.
[14] H.J. Petroski, Simple static and dynamic models for cracked elastic beams, International Journal of Fracture 17 (1972) 71–76.
[15] M.M.F. Yuen, A numerical study of the eigenparameters of a damaged cantilever beam, Journal of Sound and Vibration 103 (3) (1985) 301–310.
[16] A.D. Dimarogonas, S.A. Paipetis, Analytical Methods in Rotor Dynamics, Appl. Sci. Publishers, London, 1983, pp. 144–193.
[17] C.A. Papadopoulos, A.D. Dimarogonas, Coupling and bending of torsional vibration of cracked Timoshenko shaft, Ing. Arch. 57 (1987) 495–505.
[18] I.W. Mayes, W.G.R. Davies, A method of calculating the vibrational behaviour of coupled rotating shafts containing a transverse cracks, Paper No. C254/80, in: I. Mech. E. Conf., 1980.
[19] P. Gudmundson, Changes in modal parameters resulting from small cracks, in: Proc. 2nd Int. Modal Analysis Conf., vol. 2, Union College, Orlando, NY, USA, 1984, pp. 690–697.
[20] P.E. Rizos, N. Aspragathos, A.D. Dimarogonas, Identification of crack location and magnitude in a cantilever beam from the vibration modes, Journal of Sound and Vibration 138 (1990) 381–388.
[21] S. Loutridis, E. Douka, L.J. Hadjileontiadis, Forced vibration behaviour and crack detection of cracked beams using instantaneous frequency, NDT&E International 38 (2005) 411–419, doi:10.1016/j.ndteint.2004.11.004.
[22] S. Kitipornchai, L.L. Ke, J. Yang, Y. Xiang, Nonlinear vibration of edge cracked functionally graded Timoshenko beams, Journal of Sound and Vibration 324 (2009) 962–982, doi:10.1016/j.jsv.2009.02.023.
[23] Ugo Andreaus, Paolo Baragatti, Cracked beam identification by numerically analysing the nonlinear behaviour of the harmonically forced response, Journal of Sound and Vibration 330 (2011) 721–742, doi:10.1016/j.jsv.2010.08.032.
[24] R. Benamar, Non-linear dynamic behaviour of fully clamped beams and rectangular isotropic and laminated plates, Ph.D. thesis, University of Southampton, 1990.
[25] R. Benamar, M.M.K. Bennouna, R.G. White, The effects of large vibration amplitudes on the mode shapes and natural frequencies of thin elastic structures. Part I: Simply supported and clamped–clamped beams, Journal of Sound and Vibration 149 (1991) 179–195.
[26] R. Benamar, M.M.K. Bennouna, R.G. White, The effects of large vibration amplitudes on the mode shapes and natural frequencies of thin elastic structures. Part II: Fully clamped rectangular isotropic plates, Journal of Sound and Vibration 164 (1991) 399–424.
[27] L. Azrar, R. Benamar, R.G. White, A semi-analytical approach to the non-linear dynamic response. Problem of S–S and C–C beams at large vibration amplitudes. Part I: General theory and application to the single mode approach to free and forced vibration analysis, Journal of Sound and Vibration 224 (1999) 377–395.
[28] L. Azrar, R. Benamar, R.G. White, A semi-analytical approach to the non-linear dynamic response. Problem of beams at large vibration amplitudes. Part II: Multimode approach to the forced vibration analysis, Journal of Sound and Vibration 255 (1) (2002) 1–41, doi:10.1006/jsvi.2000.3595.
[29] L. Azrar, R. Benamar, R.G. White, Non-linear free and forced response of beams at large vibration amplitudes by a semi-analytical method, in: Proceedings of the Seventh International Conference – Structural Dynamics, Southampton, England, 2000.
[30] M. El Kadiri, R. Benamar, R.G. White, Improvement of the semi-analytical method, based on Hamilton's principle and spectral analysis, for determination of the geometrically non-linear free response of thin straight structures. Part I: Application to C–C and SS–C beams, Journal of Sound and Vibration 249 (2) (2002) 263–305.
[31] K. El Bikri, R. Benamar, M.M. Bennouna, Geometrically non-linear free vibrations of clamped simply supported rectangular plates. Part I: The effects of large vibration amplitudes on the fundamental mode shape, Comput. Struct. 81 (2003) 2029–2043.
[32] K. El Bikri, R. Benamar, M.M. Bennouna, Geometrically non-linear free vibrations of clamped–clamped beams with an edge crack, Comput. Struct. 84 (2006) 485–502, doi:10.1016/j.compstruc.2005.09.030.
[33] G.R. Irwin, Analyses of stresses and strains near the end of a crack transversing a plate, J. Appl. Mech. 24 (1957) 361–364.
[34] H. Tada, The stress analysis of cracks handbook, in: 9th Cong. Appl. Mech., Brussels, 1957.
[35] ASTM Standarts, Part 31, 1968, pp. 1018–1030.
[36] W.T. Thomson, Theory of Vibration with Applications, Prentice–Hall Inc., Englewood Cliffs, NJ, 1972.
[37] A. Eddanguir, Z. Beidouri, R. Benamar, Geometrically nonlinear transverse vibrations of discrete multi-degrees of freedom systems with a localised nonlinearity, International Journal of Mathematics and Statistics 4 (S09) (Spring 2009).